Pertanika J. Sci. & Technol. 33 (1): 241 - 259 (2025)

PERTANIKA JOURNALS

SCIENCE & TECHNOLOGY

Journal homepage: http://www.pertanika.upm.edu.my/

Acoustic Emission Partial Discharge Localization in Oil Based on Artificial Bee Colony

Zhi Yang Lim[1], Norhafiz Azis[1]*, Ahmad Hafiz Mohd Hashim[1,2], Mohd Amran Mohd Radzi[1], Nor Mohd Haziq Norsahperi[3] and Azrul Mohd Ariffin[4]

[1]Advanced Lightning, Power and Energy Research Centre (ALPER), Universiti Putra Malaysia, 43400 UPM Serdang, Selangor, Malaysia
[2]Electrical Engineering Department, German-Malaysian Institute, 43000 Kajang, Selangor, Malaysia
[3]Department of Electrical and Electronic Engineering, Universiti Putra Malaysia, 43400 UPM Serdang, Selangor, Malaysia
[4]Institute of Power Engineering, Universiti Tenaga Nasional (UNITEN), 43000 Kajang, Selangor, Malaysia

ABSTRACT

This study explores the application of an artificial bee colony (ABC) to locate partial discharge (PD) in a test tank based on acoustic emission (AE) approach. Data from a previous AE PD experimental study, which includes the coordinates of 3 AE sensors and the time difference of arrival (TDOA), were used to construct the nonlinear localization equations. It is known that localization algorithms are among the factors that can affect PD localization accuracy, and the ongoing research in this area underscores the need for further advancements in this topic. Therefore, the ABC was proposed to estimate the PD location through a colony of 120 bees, evenly divided into 60 employed and 60 onlooker bees. The employed bees explored the bounded search space, and onlooker bees refined PD locations found by the employed bees through local search. Scout bees were set out whenever a bee exceeded the limit of abandonment to discover possible PD locations in new areas of the search space. After 500 iterations, the optimal solution was the estimated PD location produced by ABC. Comparisons with the genetic algorithm (GA), particle swarm optimization (PSO) and bat algorithm (BA) revealed that the distance error, maximum deviation and computation time for AE PD localization based on ABC are the lowest. The study concludes that the ABC is more suitable for the multi-variable PD localization task than the GA, PSO, and BA due to its effective balance between local search by onlooker bees and global exploration by scout bees.

Keywords: Acoustic emission, artificial bee colony, localization, partial discharge, time difference of arrival

ARTICLE INFO

Article history:
Received: 17 April 2024
Accepted: 18 September 2024
Published: 27 January 2025

DOI: https://doi.org/10.47836/pjst.33.1.11

E-mail addresses:
gs68246@student.upm.edu.my (Zhi Yang Lim)
norhafiz@upm.edu.my (Norhafiz Azis)
ahmadhafiz@gmi.edu.my (Ahmad Hafiz Mohd Hashim)
amranmr@upm.edu.my (Mohd Amran Mohd Radzi)
nmhaziq@upm.edu.my (Nor Mohd Haziq Norsahperi)
Azrula@uniten.edu.my (Azrul Mohd Ariffin)
*Corresponding author

ISSN: 0128-7680
e-ISSN: 2231-8526

INTRODUCTION

Partial discharge (PD) can affect the integrity of power transformers since it can gradually deteriorate dielectric insulation and potentially lead to failure over time (Ilkhechi & Samimi, 2021; Liu, 2016). Therefore, PD detection and localization are crucial to maintain the reliability of power transformers (Wang et al., 2017). Conventional electrical measurement based on IEC 60270, ultra-high frequency (UHF), acoustic emission (AE) and dissolved gas analysis (DGA) are well-known methods for PD detection. PD in the insulation of a transformer results in various physical phenomena such as high-frequency electric current pulses, electromagnetic (EM) wave emissions, mechanical vibrations, chemical reactions and liberation of heat and light energies (Rathod et al., 2022). Mechanical vibrations generate AE signals, typically covering frequencies ranging from 20 kHz to 1 MHz (Rathod et al., 2022). These AE signals can be detected, denoised, and used to estimate the PD location through localization equations (Liu & Liu, 2014).

AE-based PD localization has recently gained significant attention due to its non-destructive nature (Liu, 2016). AE sensors, particularly the piezoelectric transducers, can be easily placed on the external walls of a transformer tank via magnetic holders (Hussain et al., 2021; Wang et al., 2017). AE is immune to electromagnetic interference and cost-effective (Faizol et al., 2023). However, AE is sensitive to external mechanical noise, which can introduce errors in PD localization (Al-Masri et al., 2016). It is known that the accuracy of AE PD localization relies on the localization algorithms (Liu, 2016). Iterative methods such as least square and Newton's methods are previously utilized to solve the nonlinear equations inherent in the time difference of arrival (TDOA) method for PD localization (Howells & Norton, 1981; Kundu et al., 2009; Punekar et al., 2012). These algorithms are computationally intensive and require initial guesses to perform PD localization (Howells & Norton, 1981; Kundu et al., 2009; Punekar et al., 2012). Non-iterative algorithms proposed by Kundu et al. (2009) and Antony and Punekar (2018) can provide faster computation times than Newton's method with generations of 2 solutions.

Advanced approaches such as genetic algorithm (GA) are also implemented for AE PD localization (Veloso et al., 2006, 2007, 2008). GA can estimate the PD location without any initial guesses, but it can be subjected to complicated optimization issues related to premature convergence phenomena (Liu, 2016). A quantum GA (QGA) is introduced to improve the accuracy of AE PD localization with complex computation (Liu, 2016). The bat algorithm (BA) produced less error than the QGA and GA for AE PD localization (Chakravarthi et al., 2017). The particle swarm optimization (PSO) is also utilized for AE PD localization, whereby apparent reductions of PD localization errors are found compared to the least square algorithm (Ri-cheng et al., 2008; Tang et al., 2008). Hybrid differential evolution PSO (DE-PSO) can further enhance the accuracy of AE PD localization with a longer iteration time than PSO (Cai et al., 2020). The adaptive grey wolf optimizer is

known for its ability to adjust search parameters during optimization; it also shows promise in enhancing AE PD localization (Dudani & Chudasama, 2016).

Despite these advancements, research on the algorithms for AE PD localization is still ongoing, which has prompted further study on this aspect (Dudani & Chudasama, 2016). One key challenge is balancing exploration and exploitation in the search process to avoid premature convergence and enhance PD localization accuracy. The artificial bee colony (ABC) serves as a potential candidate to address this gap since it can effectively prevent premature convergence in multi-dimensional problems, such as AE PD localization (Karaboga & Akay, 2009). Therefore, this paper presents an investigation into the application of the ABC for AE PD localization. The study aims to explore the application of ABC for AE PD localization and comprehensively compare its performance against BA, GA, and PSO. The AE PD signals used in this study are collected through 3 AE sensors placed on the surface of a steel tank filled with mineral oil. The time of arrival (TOA) for each AE PD signal is determined through the first peak method from the denoised AE PD signals (Hashim et al., 2022; Sinaga et al., 2012). Next, the TDOAs between the 3 AE signals are computed based on the TOAs. PD localizations are then carried out based on the ABC algorithm, and its performance in terms of distance error between the actual and estimated PD locations, maximum deviation of estimated PD location and average computation time is compared with BA, GA, and PSO.

METHODOLOGY

Experimental Setup and Mathematical Model of Acoustic Emission PD Localization

This study's experimental setup and data were based on the previous study (Hashim et al., 2022, 2023, 2023b). The nonlinear localization equations employed in this investigation were formulated based on the configuration shown in Figure 1, which comprised a PD source and 3 AE sensors mounted on the walls of the test tank. The spatial Cartesian coordinate system was established with one of the bottom corners of the test tank serving as the reference point, known as the origin O (0, 0, 0). The actual PD location is represented by the coordinates P (x, y, z), while the positions of the 3 AE sensors S_1, S_2, and S_3 are denoted by (x_1, y_1, z_1), (x_2, y_2, z_2), and (x_3, y_3, z_3). The needle and plane electrodes were used to create PD at 2 distinct locations in the test tank: PD location A (0.07, 0.08, 0.18 m) and PD location B (0.32, 0.09, 0.08 m), respectively. The TDOA was employed for PD localization to avoid the need to determine the actual time of arrival for the AE PD signals at each of the sensors (Liu, 2016). S_1 was specified as the reference sensor. The time difference in receiving the AE PD signals between sensor S_1 and sensor S_2, τ_{12}, was defined as $t_1 - t_2$, as depicted in Figure 2. Similarly, the difference between the arrival times of the AE PD signal at sensors S_1 and S_3 was defined as the TDOA between the 2 sensors, τ_{13}, which was mathematically expressed as $t_1 - t_3$.

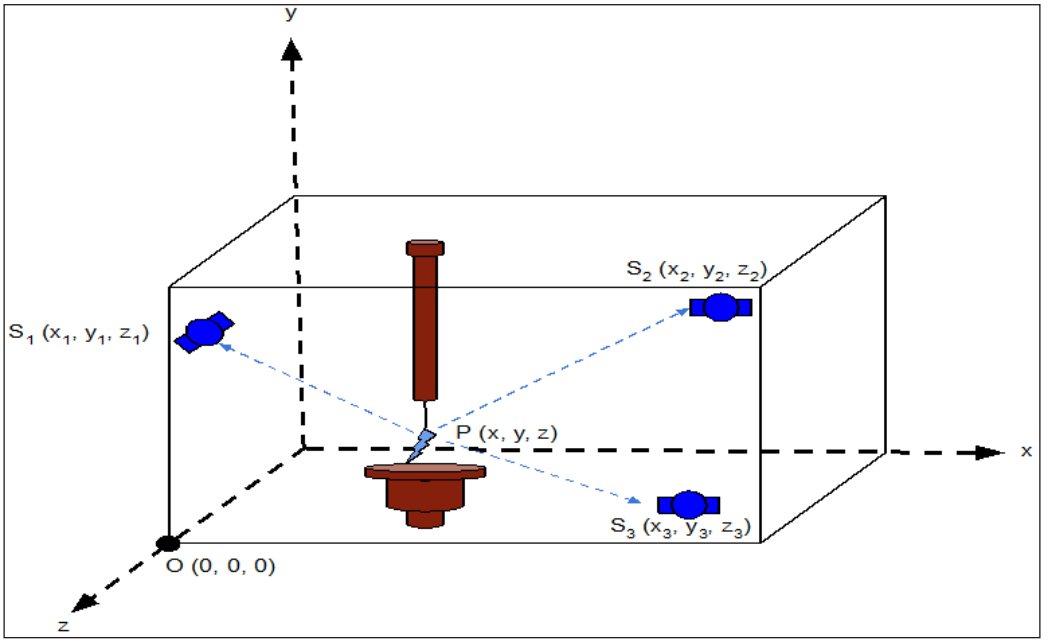

Figure 1. Schematic of AE sensors placement and actual PD location

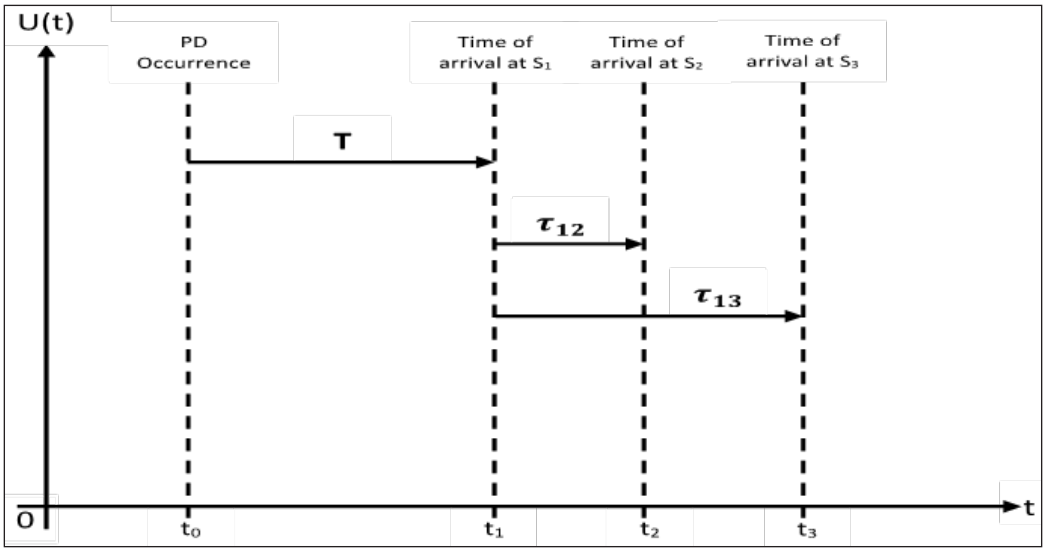

Figure 2. Difference in arrival times of acoustic emission PD signals

The system of nonlinear equations that govern the AE localization of PD in the test tank can be expressed by Equations 1, 2 and 3. These equations were obtained from the spherical distance calculations between the actual PD location and the 3 AE sensors, in

conjunction with the TDOA principles illustrated in Figure 2 (Liu, 2016; Sinaga et al., 2012; Veloso et al., 2006). The parameter v_e in these equations represented the equivalent speed of sound in oil, which was defined as 1415 m/s (Hashim et al., 2022; IEEE, 2019). Conversely, the quantity T in the equations denotes the time taken for the AE signal to travel from the actual PD location to the reference sensor S_1, which is unknown in this case.

$$(x - x_1)^2 + (y - y_1)^2 + (z - z_1)^2 = (v_e T)^2 \quad [1]$$

$$(x - x_2)^2 + (y - y_2)^2 + (z - z_2)^2 = [v_e(T + \tau_{12})]^2 \quad [2]$$

$$(x - x_3)^2 + (y - y_3)^2 + (z - z_3)^2 = [v_e(T + \tau_{13})]^2 \quad [3]$$

To reduce the number of variables to be optimized in the nonlinear localization equations, Equations 2 and 3 can be rewritten in the alternative form shown in Equation 4, whereby $i = 2, 3$ (Liu, 2016; Ri-cheng et al., 2008; Tang et al., 2008).

$$\sqrt{(x - x_i)^2 + (y - y_i)^2 + (z - z_i)^2} - \sqrt{(x - x_1)^2 + (y - y_1)^2 + (z - z_1)^2} - v_e \tau_{1i} = 0 \quad [4]$$

Equation 4 represents an over-determined situation, which indicates that the precise solution is difficult to acquire (Liu, 2016; Liu & Liu, 2014). Hence, the common approach is to seek the optimal solution of Equation 4 for AE PD localization (Liu, 2016; Liu & Liu, 2014). Overall, the mathematical model for the AE PD localization based on the TDOA can be summarized as a constrained optimization problem, as shown in Equations 5, 6, 7, and 8 (Liu, 2016; Liu & Liu, 2014; Tang et al., 2008).

$$\min\{D_f(x, y, z)\} = \sum_{i=2}^{3} \left| \sqrt{(x - x_i)^2 + (y - y_i)^2 + (z - z_i)^2} - \sqrt{(x - x_1)^2 + (y - y_1)^2 + (z - z_1)^2} - v_e \tau_{1i} \right| \quad [5]$$

subjected to

$$0 \leq x \leq (x_{\max} = 0.40 \text{ m}) \quad [6]$$

$$0 \leq y \leq (y_{\max} = 0.25 \text{ m}) \quad [7]$$

$$0 \leq z \leq (z_{max} = 0.25 \text{ m}) \quad [8]$$

Here, (x, y, z) represents the estimated PD location, (x_1, y_1, z_1) is the coordinate of the reference sensor, S_1, and (x_i, y_i, z_i) are the coordinates of the other AE sensors. For each PD location A and B, 10 combinations of AE sensor positions were used to acquire the

AE PD signal. Each combination consists of the coordinates for 3 AE sensors (S_1, S_2, and S_3), as shown in Table 1.

Table 1
Combinations of sensors for each of the PD locations

PD Location	AE Sensors Combination	AE Sensor S_1			AE Sensor S_2			AE Sensor S_3		
		x_1 (m)	y_1 (m)	z_1 (m)	x_2 (m)	y_2 (m)	z_2 (m)	x_3 (m)	y_3 (m)	z_3 (m)
A (0.07, 0.08, 0.18 m)	A1	0.15	0.10	0.00	0.15	0.05	0.00	0.15	0.15	0.00
	A2	0.20	0.10	0.25	0.20	0.05	0.25	0.20	0.15	0.25
	A3	0.25	0.05	0.00	0.25	0.15	0.00	0.35	0.10	0.00
	A4	0.25	0.05	0.00	0.30	0.10	0.00	0.35	0.15	0.00
	A5	0.25	0.15	0.25	0.25	0.05	0.25	0.25	0.10	0.25
	A6	0.30	0.15	0.25	0.30	0.05	0.25	0.30	0.10	0.25
	A7	0.40	0.05	0.20	0.40	0.10	0.10	0.40	0.15	0.20
	A8	0.40	0.05	0.20	0.40	0.15	0.15	0.40	0.05	0.10
	A9	0.40	0.15	0.10	0.40	0.15	0.20	0.40	0.05	0.15
	A10	0.40	0.15	0.15	0.40	0.05	0.15	0.40	0.10	0.05
B (0.33, 0.09, 0.08 m)	B1	0.00	0.05	0.05	0.00	0.15	0.05	0.00	0.10	0.15
	B2	0.15	0.05	0.25	0.15	0.15	0.25	0.05	0.10	0.25
	B3	0.20	0.15	0.25	0.20	0.10	0.25	0.15	0.15	0.25
	B4	0.25	0.05	0.00	0.20	0.15	0.00	0.15	0.05	0.00
	B5	0.25	0.05	0.25	0.00	0.05	0.10	0.15	0.15	0.00
	B6	0.25	0.10	0.25	0.15	0.05	0.25	0.15	0.15	0.25
	B7	0.30	0.10	0.00	0.15	0.05	0.00	0.10	0.15	0.00
	B8	0.35	0.15	0.00	0.40	0.15	0.10	0.35	0.15	0.25
	B9	0.40	0.05	0.05	0.20	0.15	0.00	0.00	0.05	0.20
	B10	0.40	0.05	0.10	0.35	0.05	0.00	0.15	0.10	0.25

Implementation of Optimization Algorithms for PD Localization

To assess the performance of the ABC for AE PD localization, GA, PSO and BA were also applied to solve the same optimization problem for comparative analysis (Chakravarthi et al., 2017; Ri-cheng et al., 2008; Tang et al., 2008; Veloso et al., 2006). For each algorithm, Equation 5 serves as the objective function for the AE PD localization. Equations 6, 7 and 8 define a 3-dimensional search space that confines the estimated PD locations produced by each algorithm. This confined search space represents the actual dimension of the experimental test tank. The AE sensors' coordinates (x_i, y_i, z_i) and reference sensor coordinates (x_1, y_1, z_1) were pre-defined and listed in Table 1. The detailed processes to obtain the TDOAs used in this study were outlined in (Hashim et al., 2022). Table 2 shows the TDOAs for each AE sensor combination in Table 1. The optimal solution for each algorithm is the estimated PD location for the given combinations of TDOAs and AE sensors' coordinates.

Table 2
TDOAs for the combinations of AE sensors in Table 1

PD Location	AE Sensors Combination	TDOA, τ_{12} (μs)	TDOA, τ_{13} (μs)
A (0.07, 0.08, 0.18 m)	A1	1.237	7.449
	A2	1.406	9.943
	A3	4.883	54.155
	A4	25.420	58.664
	A5	1.081	7.774
	A6	0.876	6.318
	A7	-0.148	5.703
	A8	4.459	6.318
	A9	1.000	10.000
	A10	3.000	15.594
B (0.33, 0.09, 0.08 m)	B1	5.000	4.000
	B2	4.999	54.000
	B3	6.000	29.000
	B4	34.000	59.000
	B5	0.000	5.997
	B6	41.000	45.000
	B7	75.000	115.000
	B8	0.000	61.000
	B9	50.000	189.000
	B10	8.000	118.000

Genetic Algorithm

A real-coded GA was implemented for the AE PD localization with reference to (Veloso et al., 2006, 2007). Hence, the genes for all 120 chromosomes in the population are real numbers. The important parameters that are used in GA are summarized in Table 3. The GA started with the random initializations of 120 chromosomes. Each chromosome consists of 3 genes representing the (*x, y, z*) coordinates of the estimated PD locations.

To estimate the PD location for each of the AE sensor combinations in Table 1, the coordinates of the 3 AE sensors (x_i, y_i, z_i), along with the corresponding TDOAs in Table 2 (τ_{1i}), were used as inputs for the GA. The AE PD signals captured by the AE sensors during the PD experiment were first denoised by the moving average (MA) technique (Hashim et al., 2022; Hashim et al., 2023b). The TOAs of the 3 AE sensors were then determined from the denoised AE PD signals based on the first peak method (Hashim et al., 2022; Sinaga et al., 2012). These TOAs represent the moments when the AE PD signals emitted from the actual PD location arrive at the respective AE sensors. The TDOAs were computed based on the concept illustrated in Figure 2. For AE PD localization, the cost value for each chromosome was obtained by substituting the 3 genes in each chromosome

into the objective function of the GA, given by Equation 5. A total of 500 generations of chromosomes were produced. In each generation, 84 new chromosomes were produced through the crossovers among 42 pairs of selected parent chromosomes. The probability of each chromosome being selected as a parent through the roulette wheel selection was computed based on Equation 9, where $cost_i$ is the cost of the ith chromosome obtained from the objective function (Heris, 2015).

$$P = e^{-0.8\times\left(\frac{cost_i}{worst\ \ cost\ \ value\ \ of\ \ the\ generation}\right)} \quad [9]$$

The exponential conversion in Equation 9 assigned a higher probability of selection to chromosomes with smaller absolute cost values and vice versa. The smaller the absolute cost value of a chromosome, the closer the estimated PD location that is represented by the genes of the chromosomes to the actual PD location. Furthermore, 36 new chromosomes were produced through creep-type mutation of 36 chromosomes in the current generation. The mutation operation enabled GA to explore different locations in the test tank for the estimated PD location by injecting diversity into the gene pool. Next, the 120 chromosomes generated by crossover and mutation operations were merged with the existing chromosome population. Elitism was applied whereby only 120 chromosomes with the best cost values were retained to constitute the subsequent generation. This selective retention strategy ensured that each successive generation of chromosomes comprised estimated PD locations with higher probabilities of proximity to the actual PD location. After the elitism process, the GA proceeded with the next iteration. The output of the GA was obtained from the best chromosome in the 500th generation. The 3 genes of this best chromosome resulted in the lowest absolute cost value when substituted into the objective function. It means that the estimated PD location (x, y, z) represented by the genes was closest to the actual PD location in the test tank.

Table 3
Parameters of the GA for acoustic emission PD localization

Parameter	Value
Size of the population	120
Maximum number of generations	500
Probability of mutation	0.05
Percentage of offspring produced by crossover (%)	70
Percentage of offspring produced by mutation (%)	30

Particle Swarm Optimization Algorithm

A standard PSO was employed for the AE PD localization based on the methodology outlined in (Ri-cheng et al., 2008; Tang et al., 2008). All parameters of the PSO were set

the same as in (Ri-cheng et al., 2008; Tang et al., 2008), except for the inertia factor or the inertia weight, denoted by w. Initially, the inertia weight was set to 1 and reduced in every subsequent iteration based on Equation 10, with the damping factor, w_{damp}, held constant at 0.99 (Heris, 2015). The crucial parameters the PSO needs to perform the AE PD localization task are tabulated in Table 4.

Equation 5 was employed as the objective function of the PSO to predict the actual PD location within the test tank. The coordinates of the 3 AE sensors (x_i, y_i, z_i) listed in Table 1 served as the inputs to the PSO. The corresponding TDOAs, listed in Table 2, were also utilized as inputs to the PSO to estimate the actual PD location based on Equation 5. In each iteration of the PSO, each swarm particle's velocity and location were updated based on the same equations given in (Ri-cheng et al., 2008; Tang et al., 2008). The output of the PSO was obtained from the g_{Best} parameter, which was updated whenever a particle found an estimated PD location closer to the actual PD location than the previously recorded best location. This parameter contained the (x, y, z) coordinates of the estimated PD location nearest to the actual PD location, as found by the particles in the swarm.

$$w(k+1) = w(k) \times w_{damp} \quad [10]$$

Table 4
Parameters of the PSO for acoustic emission PD localization

Parameter	Value
Size of particle swarm	120
Maximum number of iterations	500
Initial inertia factor (w_0)	1
The damping factor of inertia factor (w_{damp})	0.99
Personal learning factor (C_1)	2
Global learning factor (C_2)	2

Bat Algorithm

The AE PD localization based on BA was implemented according to the procedures in (Chakravarthi et al., 2017; Yang, 2010).. The important parameters of the BA for AE PD localization are summarized in Table 5. The locations of the bats represented the estimated PD locations based on BA in the confined search space defined by Equations 6, 7, and 8. This confined search space restricted the movements of the bats so that the estimated PD locations produced by the BA were always within the test tank. The BA can be regarded as a modified version of PSO with additional parameters involved in the search for the actual PD location. These parameters included the velocity (v_i), pulse frequency (f_i), pulse emission rate (r_i), and loudness (A_i) for each of the bats in the population (Chakravarthi et

al., 2017; Yang, 2010). These parameters were computed and updated in each iteration of the BA based on the equations provided by Chakravarthi et al. (2017) and Yang (2010). Equation 5 serves as the objective function of the BA for AE PD localization. The inputs of the BA included the coordinates of the 3 AE sensors (x_i, y_i, z_i) as listed in Table 1 and the corresponding TDOAs given in Table 2. The cost value for each bat in the population was obtained by substituting the 3 coordinates in the bat's location into the objective function. A small absolute cost value indicates that the bat's location is relatively closer to the actual PD location. Therefore, the bat's location with the lowest absolute cost value in the population represents the estimated PD location closest to the actual PD location in terms of the Euclidean distance. The output of the BA was taken from the best bat location identified in the bat population over 500 iterations of computation.

Table 5
Parameters of the BA for acoustic emission PD localization

Parameter	Value
Size of the bat population	120
Maximum number of iterations	500
The frequency range of each bat [f_{min},f_{max}]	[0, 1.5]
Initial loudness of each bat (A_0)	1
Initial pulse emission rate (r_0)	0.6
Loudness decay constant (α)	0.9
Pulse emission rate constant (γ)	0.9

Artificial Bee Colony Algorithm

An ABC was implemented for AE PD localization with reference to (Karaboga, 2005; Karaboga & Akay, 2009; Kulkarni & Desai, 2016). The bee colony utilized 120 bees, divided into 60 employed and 60 onlooker bees. The group of employed bees was tasked to search for certain locations within the confined 3-dimensional search space defined by Equations 6, 7, and 8 for the actual location of PD. The bee's location, represented by 3 coordinates (x, y, z), together with the coordinates of the AE sensors in Table 1 and the corresponding TDOAs in Table 2, were set as inputs for the objective function given by Equation 5. These TDOAs were computed from the differences among the TOAs of the AE PD signals acquired by each AE sensor.

The output from the objective function was the cost value of the bee. It indicates how close the location of a bee is to the actual PD location, whereby the lower the absolute cost value of a bee is, the closer its location is to the actual PD location. The onlooker bees were employed to perform local searches around the locations of the employed bees with higher fitness values. The fitness values of the employed bees were computed based

on Equation 11, which assigned a higher fitness value for a bee with a lower absolute cost value and vice versa (Kulkarni & Desai, 2016). In Equation 11, f_i and c_i represented each employed bee's fitness and cost values, respectively. Subsequently, a greedy selection process was executed to determine whether to retain the employed bee's location or replace it with the onlooker bee's location based on the proximity of the 2 locations to the actual PD location. Each bee in the colony was assigned a crucial parameter known as the limit of abandonment (Karaboga, 2005; Karaboga & Akay, 2009). This parameter was increased by 1 whenever the greedy selection process resulted in no replacement of a bee's location, and it was reset to 0 once a replacement occurred. Once a bee exceeded its limit of abandonment, it was sent out as a scout bee to explore new areas within the confined search space to pinpoint the actual PD location. The transition of a bee into a scout indicated that the vicinity of the bee's location was adequately examined, without any new location found to be closer to the actual PD location than the bee's current location. In this study, the limit of abandonment for the bees was set to 180 based on Equation 12 (Karaboga & Akay, 2009), where $N_{employed\_bees}$ is the number of employed bees in the colony, and D represents the dimension of the AE PD localization problem, which in this case is 3. At the end of each iteration, the location of the bee with the lowest absolute cost value in the current iteration was compared to the best location identified by the bee colony, denoted as g_{Best}. This comparison was made to ascertain if the current best location was closer to the actual PD location than the previously established best location, g_{Best} . Specifically, g_{Best} was updated only if the absolute cost value of the newly discovered best location in the current iteration proved to be smaller than that of g_{Best}. The ABC was terminated upon completing 500 iterations, and the output was the 3 coordinates (x, y, z) of the estimated PD location in the g_{Best} parameter. The important parameters used for the ABC are tabulated in Table 6.

$$f_i = \begin{cases} \frac{1}{1+c_i}, if\ c_i \geq 0 \\ \frac{1}{1+|c_i|}, if\ c_i < 0 \end{cases} \quad [11]$$

$$Limit = N_{employed\_bees} \times D \quad [12]$$

Table 6
Parameters of the ABC for acoustic emission PD localization

Parameter	Value
Size of bee colony	120
Maximum number of iterations	500
Limit of abandonment	180

PD Localization Analysis

To ensure a fair comparison, all four algorithms employed in this study were carried out over 500 iterations with 120 search agents in each population. For each of the estimated PD locations, the distance error and the maximum deviation were computed based on Equations 13 and 14, respectively (Chakravarthi et al., 2017; Dudani & Chudasama, 2016; Liu, 2016). ΔR in Equation 13 represents the distance error between the estimated PD and actual PD locations based on the Euclidean distance (Hashim et al., 2022). x_{act}, y_{act} and z_{act} in Equations 13 and 14 represent the actual PD location in the test tank, whereas x_{cal}, y_{cal} and z_{cal} signify the estimated PD location by each algorithm. The maximum deviation is denoted by , as shown in Equation 14.

$$\Delta R = \sqrt{(x_{act} - x_{cal})^2 + (y_{act} - y_{cal})^2 + (z_{act} - z_{cal})^2} \quad [13]$$

$$D_{max} = \max\begin{Bmatrix} |x_{act} - x_{cal}| \\ |y_{act} - y_{cal}| \\ |z_{act} - z_{cal}| \end{Bmatrix} \quad [14]$$

RESULTS AND DISCUSSION

Figures 3 and 4 show the PD localizations based on the GA, PSO, BA, and ABC for PD locations A and B, respectively. Each of the estimated PD locations represents the mean of 20 estimates obtained from 20 independent applications for each algorithm. According to the Figures 3 and 4, the estimated PD locations based on ABC are the closest to the actual PD location, followed by BA, PSO and GA.

The ABC consistently demonstrates the highest PD localization accuracy regardless of the arrangement of AE sensors and PD locations A and B, as shown in Figures 5(a) and 5(b). The good balance among the local search mechanism that is provided by the artificial onlooker and employed bees and the global exploration process that is managed by the scout bees allows the ABC to produce good results for the multi-variable PD localization task, with the lowest average distance errors of 0.0481 m for PD location A and 0.0959 m for PD location B (Karaboga & Akay, 2009). In terms of Euclidean distance, the average distance error for PD location A that the ABC obtained is 37.04%, 55.55%, and 48.61% lower than the BA, PSO, and GA, respectively. For PD location B, the average distance error that the ABC produces is 32.27%, 43.15%, and 51.61% lower than the BA, PSO, and GA. Apart from the ABC, the BA performs better than the GA and PSO for the AE PD localization at PD locations A and B, which is a constrained optimization problem (Yang, 2010). It is evident from Figure 5(a) for PD location A, where the average distance error of the estimated PD location by BA is 0.0764 m, which is 29.39% and 18.38% lower than the PSO and GA, respectively. Similarly, from Figure 5(b), the average distance error of the

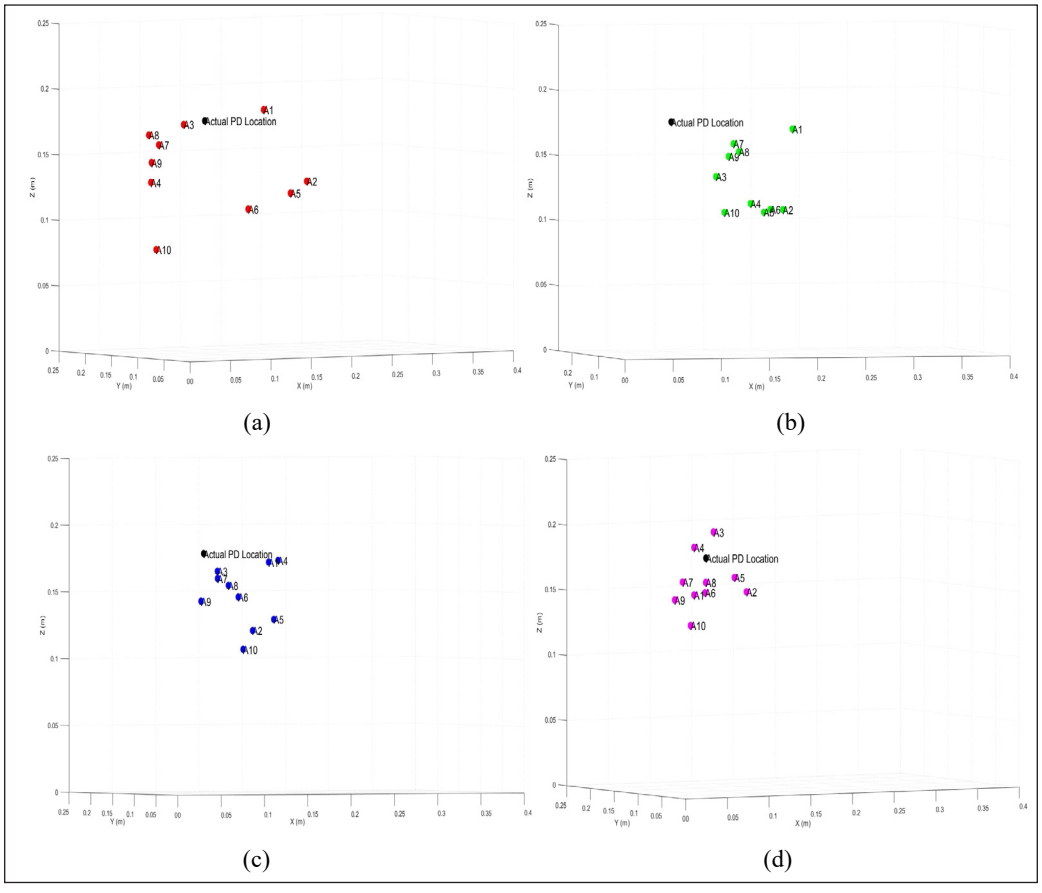

Figure 3. PD localization for PD location A based on (a) GA (red); (b) PSO (green); (c) BA (blue); (d) ABC (purple)

estimated PD locations for PD location B by BA is 0.1416 m, which is 16.06% and 28.55% lower than the PSO and GA, respectively. The PD localization accuracies of GA and PSO show inconsistency for both PD locations A and B, possibly due to the implementation of probabilistic modeling to change a part of the existing solutions in the search for a better estimated PD location (Karaboga & Akay, 2009; Kulkarni & Desai, 2016). For PD location A, the GA demonstrates more effective exploration and exploitation of the search space than PSO. The average distance error of the estimated PD locations by GA is 0.0936 m, which is 13.50% lower than that produced by the PSO. The PSO showcases a better ability to avoid local convergence and better global search ability for the cases of PD location B because the average distance error of the estimated PD locations produced by the PSO is 0.1687 m, which is 14.88% lower than the GA. The PD locations estimated by both the GA and PSO for both PD locations A and B are farther away from the actual PD location as compared to the ABC, most likely because of the local convergence problem (Karaboga & Akay, 2009; Kulkarni & Desai, 2016; Tang et al., 2008).

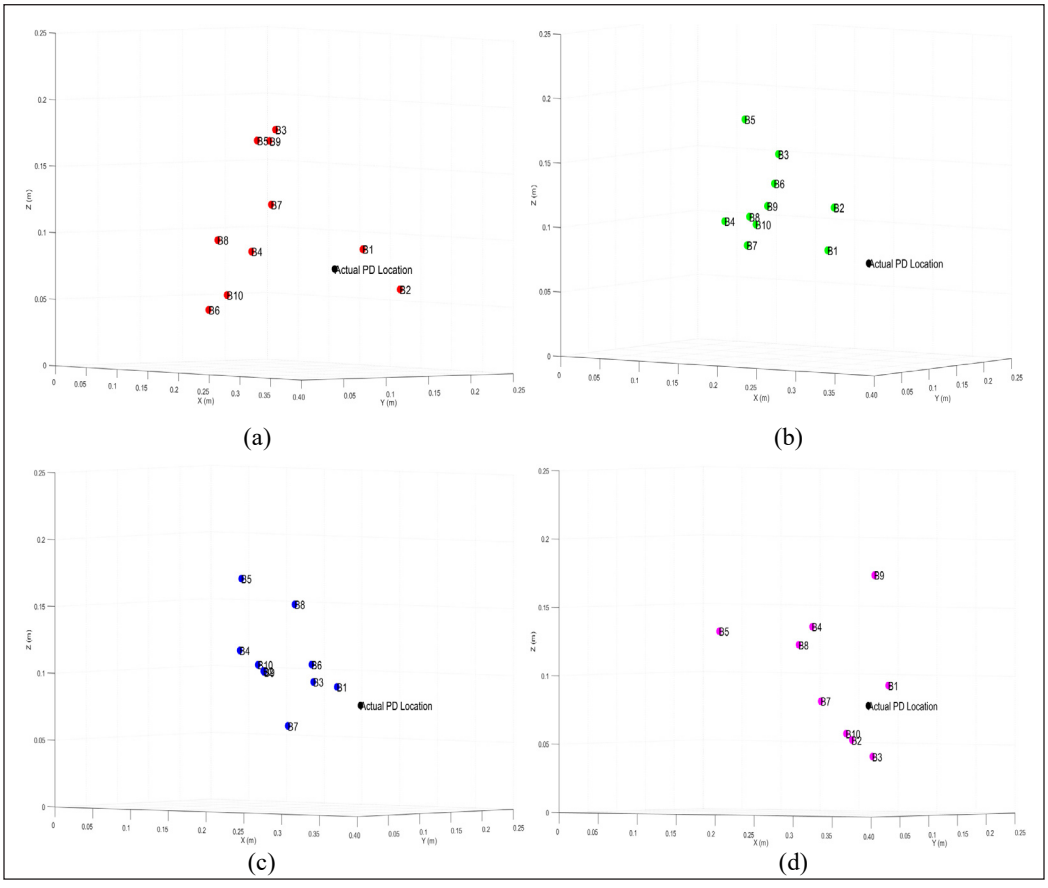

Figure 4. PD localization for PD location B based on (a) GA (red); (b) PSO (green); (c) BA (blue); (d) ABC (purple)

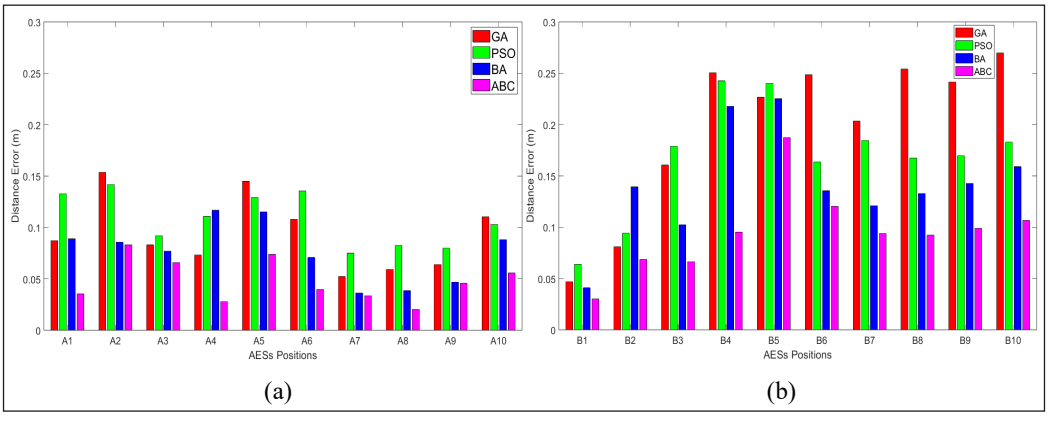

Figure 5. Distance errors of the estimated PD locations by GA, PSO, BA, and ABC for (a) Location A and (b) Location B

The maximum deviations of the estimated PD locations based on the ABC for PD location A are between 0.019 m and 0.069 m, as shown in Figure 6(a). For PD location B, the maximum deviations of the estimated PD locations based on the ABC are from 0.026 m to 0.179 m, as illustrated in Figure 6(b). Based on the BA, the maximum deviations of the estimated PD locations are from 0.025 m to 0.108 m for PD location A and from 0.038 m to 0.207 m for PD location B. The maximum deviations of the estimated PD locations based on the PSO are between 0.061 m to 0.131 m for PD location A and between 0.062 m and 0.232 m for PD location B, as depicted in Figures 6(a) and 6(b). For PD location A, the maximum deviation range for the estimated PD locations based on the GA is from 0.046 m to 0.143 m. On the other hand, for PD location B, the maximum deviation range for the estimated PD locations based on GA is from 0.044 m to 0.261 m. For PD location A, the average of the maximum deviations of the estimated PD locations produced by the ABC algorithm is 0.0387 m, which is 38.77%, 57.14%, and 51.38% lower than the BA, PSO, and GA. For PD location B, the average value of the maximum deviations of the estimated PD locations based on the ABC is 0.0818 m, which is 37.70%, 47.53%, and 48.23% lower than the BA, PSO, and GA. These findings indicate that the estimated PD locations produced by the ABC deviate less from the actual PD location as compared to the BA, PSO, and GA. This consistency in the average of the maximum deviations aligns with the findings of the average distance errors, which highlight the good accuracy and reliability of the ABC for PD localization as compared to the other algorithms.

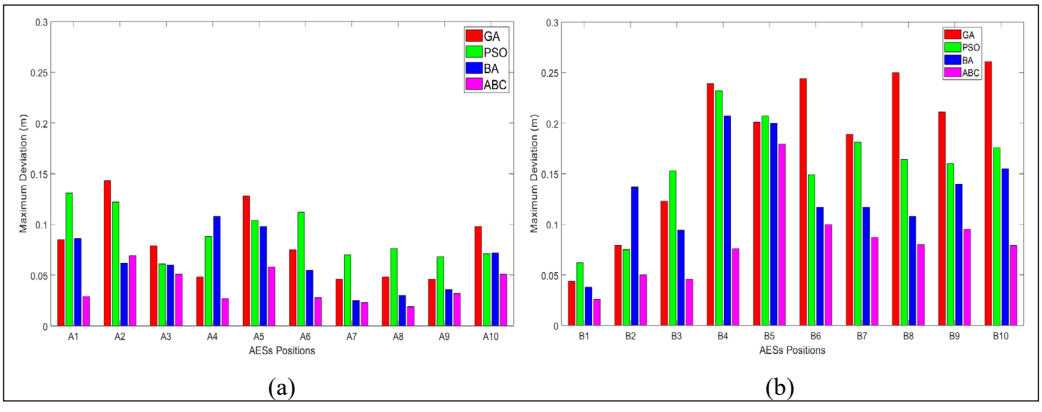

Figure 6. Maximum deviation of the estimated PD locations by GA, PSO, BA, and ABC for (a) PD Location A and (b) PD Location B

The average computation times for the GA, PSO, BA, and ABC to estimate the PD locations for PD location A are presented in Figure 7(a). Each average computation time in Figures 7(a) and 7(b) represents the mean value of 20 computation times for each AE sensor combination. The average computation time for the ABC is the shortest, with an

average of 0.7556 s. For PD location A, the average computation time by BA is 0.88 s, which outperforms GA, with 1.1509 s and PSO, with 0.9195 s. A similar trend is observed in Figure 7(b) whereby for PD location B, the average computation time for ABC is the fastest with 0.7713 s followed by BA, PSO and GA with 0.8965 s, 0.9375 s and 1.1486 s, respectively. Overall, the ABC takes the shortest time to estimate the PD locations for both PD locations A and B. For PD location A, the average computation time of the ABC is 14.13%, 17.83%, and 34.35% faster than the BA, PSO, and GA. For PD location B, the average computation time of the ABC is 13.97%, 17.73%, and 32.85% faster than the BA, PSO, and GA. The ABC's fastest average computation time to obtain an estimated PD location is probably attributed to its inherent advantage. This advantage stems from the fact that ABC has only 1 control parameter, which is the limit for abandonment. In comparison, other algorithms such as GA, PSO, and BA have at least 2 parameters to be updated for the computation (Karaboga & Akay, 2009).

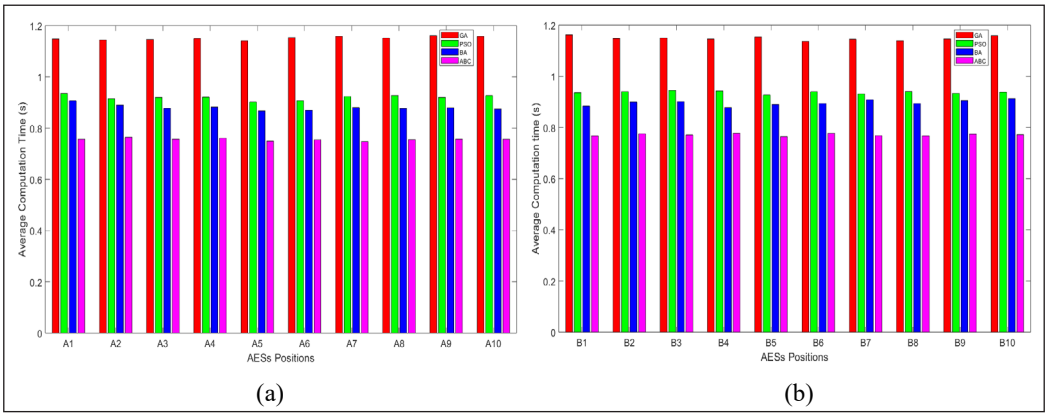

Figure 7. The average computation time of GA, PSO, BA, and ABC for (a) PD Location A and (b) PD Location B

CONCLUSION

In conclusion, it is found that the ABC outperforms the BA, GA, and PSO in AE PD localization regardless of the AE sensor arrangements and PD locations within the test tank. The distance errors between estimated and actual PD locations by ABC range from 0.0202 m to 0.0831 m for PD location A and from 0.0300 m to 0.1875 m for PD location B, representing the smallest errors obtained in the study. The high PD localization accuracy of the ABC is attributed to its effective search mechanism, which balances local search by onlooker bees with global exploration by scout bees. The ABC exhibits the shortest average computation time to estimate the PD locations in 500 iterations by optimizing the nonlinear localization equations. This is likely due to the algorithm's inherent advantage of requiring only one control parameter. The BA performs better than the GA and PSO, with relatively

lower distance errors for AE PD localization and shorter computation time to obtain the estimated PD locations. GA and PSO show inconsistency in PD localization accuracy, but the average computation time needed by the PSO to give estimated PD locations is shorter than that of the GA. While the ABC shows promise in AE PD localization, its performance might vary with different types and levels of noises or interferences during on-site testing. Future studies could address this by testing the algorithm under different noise conditions and more complex scenarios, such as accounting for the effect of temperature, moisture and pressboard.

ACKNOWLEDGMENTS

This research was funded by Universiti Putra Malaysia Inisiatif Putra Berkumpulan GP-IPB (GP-IPB/2022/9717000) funding scheme.

REFERENCES

Al-Masri, W. M. F., Abdel-Hafez, M. F., & El-Hag, A. H. (2016). Toward high-accuracy estimation of partial discharge location. *IEEE Transactions on Instrumentation and Measurement*, *65*(9), 2145–2153. https://doi.org/10.1109/TIM.2016.2573098

Antony, D., & Punekar, G. S. (2018). Noniterative method for combined acoustic-electrical partial discharge source localization. *IEEE Transactions on Power Delivery*, *33*(4), 1679–1688. https://doi.org/10.1109/TPWRD.2017.2769159

Cai, J., Zhou, L., Hu, J., Zhang, C., Liao, W., & Guo, L. (2020). High-accuracy localisation method for PD in transformers. *IET Science, Measurement & Technology*, *14*(1), 104–110. https://doi.org/10.1049/iet-smt.2019.0051

Chakravarthi, M. K., Giridhar, A. V., & Sarma, D. V. S. S. S. (2017, December 21-23). *Localization of partial discharge source in power transformer using bat algorithm*. [Paper presentation]. 7th International Conference on Power Systems (ICPS), Pune, India. https://doi.org/10.1109/ICPES.2017.8387324

Dudani, K., & Chudasama, A. R. (2016). Partial discharge detection in transformer using adaptive grey wolf optimizer based acoustic emission technique. *Cogent Engineering*, *3*(1), Article 1256083. https://doi.org/10.1080/23311916.2016.1256083

Faizol, Z., Zubir, F., Saman, N. M., Ahmad, M. H., Rahim, M. K. A., Ayop, O., Jusoh, M., Majid, H. A., & Yusoff, Z. (2023). Detection method of partial discharge on transformer and gas-insulated switchgear: A review. *Applied Sciences*, *13*(17), Article 9605. https://doi.org/10.3390/app13179605

Hashim, A. H. M., Azis, N., Jasni, J., Radzi, M. A. M., Kozako, M., Jamil, M. K. M., & Yaakub, Z. (2023a). Application of ANFIS and ANN for partial discharge localization in oil through acoustic emission. *IEEE Transactions on Dielectrics and Electrical Insulation*, *30*(3), 1247–1254. https://doi.org/10.1109/TDEI.2023.3264958

Hashim, A. H. M., Azis, N., Jasni, J., Radzi, M. A. M., Kozako, M., Jamil, M. K. M., & Yaakub, Z. (2023b). Examination on the denoising methods for electrical and acoustic emission partial discharge signals in

oil. *Indonesian Journal of Electrical Engineering and Informatics (IJEEI)*, *11*(3), 791–804. https://doi.org/10.52549/ijeei.v11i3.4463

Hashim, A. H. M., Azis, N., Jasni, J., Radzi, M. A. M., Kozako, M., Jamil, M. K. M., & Yaakub, Z. (2022). Partial discharge localization in oil through acoustic emission technique utilizing fuzzy logic. *IEEE Transactions on Dielectrics and Electrical Insulation*, *29*(2), 623-630. https://doi.org/10.1109/TDEI.2022.3157911

Heris, M. (2015). *Binary and real-coded genetic algorithms*. MATLAB Central File Exchange.

Heris, M. (2015). *Particle swarm optimization (PSO)*. MATLAB Central File Exchange.

Howells, E. T. N. E., & Norton, E. T. (1981). Location of partial discharge sites in on-line transformers. *IEEE Transactions on Power Apparatus and Systems*, *100*(1), 158-162. https://doi.org/10.1109/TPAS.1981.316872

Hussain, M. R., Refaat, S. S., & Abu-Rub, H. (2021). Overview and partial discharge analysis of power transformers: A literature review. *IEEE Access*, *9*, 64587–64605. https://doi.org/10.1109/ACCESS.2021.3075288

IEEE. (2019). *C57.127-2018 - IEEE Guide for the Detection, Location and Interpretation of Sources of Acoustic Emissions from Electrical Discharges in Power Transformers and Power Reactors*. IEEE. https://doi.org/10.1109/IEEESTD.2019.8664690

Ilkhechi, H. D., & Samimi, M. H. (2021). Applications of the acoustic method in partial discharge measurement: A review. *IEEE Transactions on Dielectrics and Electrical Insulation*, *28*(1), 42–51. https://doi.org/10.1109/TDEI.2020.008985

Karaboga, D. (2005). *An idea based on honey bee swarm for numerical optimization* (Technical Report - TR06). Erciyes University. chrome-extension://efaidnbmnnnibpcajpcglclefindmkaj/https://abc.erciyes.edu.tr/pub/tr06_2005.pdf

Karaboga, D., & Akay, B. (2009). A comparative study of Artificial Bee Colony algorithm. *Applied Mathematics and Computation*, *214*(1), 108–132. https://doi.org/10.1016/j.amc.2009.03.090

Kulkarni, V. R., & Desai, V. (2016, December 15-17). *ABC and PSO: A comparative analysis*. [Paper presentation]. IEEE International Conference on Computational Intelligence and Computing Research (ICCIC), Chennai, India. https://doi.org/10.1109/ICCIC.2016.7919625

Kundu, P., Kishore, N. K., & Sinha, A. K. (2009). A non-iterative partial discharge source location method for transformers employing acoustic emission techniques. *Applied Acoustics*, *70*(11–12), 1378–1383. https://doi.org/10.1016/j.apacoust.2009.07.001

Liu, H. L. (2016). Acoustic partial discharge localization methodology in power transformers employing the quantum genetic algorithm. *Applied Acoustics*, *102*, 71–78. https://doi.org/10.1016/j.apacoust.2015.08.011

Liu, H. L., & Liu, H. D. (2014). Partial discharge localization in power transformers based on the sequential quadratic programming-genetic algorithm adopting acoustic emission techniques. *EPJ Applied Physics*, *68*(1), Article 10801. https://doi.org/10.1051/epjap/2014140318

Punekar, G. S., Jadhav, P., Bhavani, S. T., & Nagamani, H. N. (2012, July 24-28). *Some aspects of location identification of PD source using AE signals by an iterative method*. [Paper presentation]. IEEE 10th

International Conference on the Properties and Applications of Dielectric Materials, Bangalore, India. https://doi.org/10.1109/ICPADM.2012.6318957

Rathod, V. B., Kumbhar, G. B., & Bhalja, B. R. (2022). Partial discharge detection and localization in power transformers based on acoustic emission: Theory, methods, and recent trends. *IETE Technical Review*, *39*(3), 540-552. https://doi.org/10.1080/02564602.2021.1871672

Ri-cheng, L., Kai, B., Chun, D., Shao-yu, L., & Guo-zheng, X. (2008, November 9-12). *Study on partial discharge localization by ultrasonic measuring in power transformer based on particle swarm optimization*. [Paper presentation]. International Conference on High Voltage Engineering and Application, Chongqing, China. https://doi.org/10.1109/ICHVE.2008.4774007

Sinaga, H. H., Phung, B. T., & Blackburn, T. R. (2012). Partial discharge localization in transformers using UHF detection method. *IEEE Transactions on Dielectrics and Electrical Insulation*, *19*(6), 1891-1900. https://doi.org/10.1109/TDEI.2012.6396945

Tang, L., Luo, R., Deng, M., & Su, J. (2008). Study of partial discharge localization using ultrasonics in power transformer based on particle swarm optimization. *IEEE Transactions on Dielectrics and Electrical Insulation*, *15*(2), 492–495. https://doi.org/10.1109/TDEI.2008.4483469

Veloso, G. C., Silva, L. E. B. D., Lambert-Torres, G., & Pinto, J. O. P. (2006). Localization of partial discharges in transformers by the analysis of the acoustic emission. In *IEEE International Symposium on Industrial Electronics* (pp. 537–541). IEEE Publishing. https://doi.org/10.1109/ISIE.2006.295515

Veloso, G. F. C., Silva, L. E. B. D., & Lambert-Torres, G. (2007). A strategy to locate partial discharges in power transformers using acoustic emission. *Renewable Energy and Power Quality Journal*, *1*(5), 596–600. https://doi.org/10.24084/repqj05.344

Veloso, G. F. C., Silva, L. E. B. D., Noronha, I., & Lambert-Torres, G. (2008, June 30 – July 2). *Identification of wavefronts in Partial Discharge acoustic signals using discrete wavelet transform*. [Paper presentation]. IEEE International Symposium on Industrial Electronics, Cambridge, United Kingdom. https://doi.org/10.1109/ISIE.2008.4677219

Wang, Y. B., Chang, D. G., Fan, Y. H., Zhang, G. J., Zhan, J. Y., Shao, X. J., & He, W. L. (2017). Acoustic localization of partial discharge sources in power transformers using a particle-swarm-optimization-route-searching algorithm. *IEEE Transactions on Dielectrics and Electrical Insulation*, *24*(6), 3647–3656. https://doi.org/10.1109/TDEI.2017.006857

Yang, X. S. (2010). *A new metaheuristic bat-inspired algorithm*. In J. R. Gonzalex, D. A. Pelta, C. Cruz, G. Terrazas & N. Krasnogpr (Eds.) *Nature inspired cooperative strategies for optimization* (pp. 65–74). Springer. https://doi.org/10.1007/978-3-642-12538-6_6